DRAFT VERSION APRIL 10, 2009
Preprint typeset using LaTeX style emulateapj v. 02/07/07

A NECESSARY CONDITION FOR INDIVIDUAL TIME-STEPS IN SPH SIMULATIONS

TAKAYUKI R.SAITOH[1], JUNICHIRO MAKINO[1,2]

(Received 2008 Aug 5; Accepted 2009 Apr 9)
Draft version April 10, 2009

ABSTRACT

We show that the smoothed particle hydrodynamics (SPH) method, used with individual time-steps in the way described in the literature, cannot handle strong explosion problems correctly. In the individual time-step scheme, particles determine their time-steps essentially from a local Courant condition. Thus they cannot respond to a strong shock, if the pre-shock timescale is too long compared to the shock timescale. This problem is not severe in SPH simulations of galaxy formation with a temperature cutoff in the cooling function at 10^4 K, while it is very dangerous for simulations in which the multiphase nature of the interstellar medium under 10^4 K is taken into account. A solution for this problem is to introduce a time-step limiter which reduces the time-step of a particle if it is too long compared to the time-steps of its neighbor particles. Thus this kind of time-step constraint is essential for the correct treatment of explosions in high-resolution SPH simulations with individual time-steps.

Subject headings: galaxies:evolution—galaxies:ISM—galaxies:star formation—methods:numerical

1. INTRODUCTION

Hierarchical (individual) time-step method (e.g., McMillan 1986; Hernquist & Katz 1989; Makino 1991a) is widely used in simulations of galaxy formation and star formation based on smoothed particle hydrodynamics (SPH) method (Lucy 1977; Gingold & Monaghan 1977). This method allows particles to have different time-steps, and can significantly reduce the total calculation cost when there is a large variation in the timescales of particles. Almost all implementations of the individual time-steps method used for particle systems violates Newton's third law (see Farr & Bertschinger 2007 for one of exception). As long as physical quantities are integrated with sufficient accuracy, this violation is not a severe problem.

However, it is not always possible to maintain the accuracy. To our knowledge, all existing implementations of individual time-step for SPH rely on the determination of the time-step at the end of previous time-steps. Therefore, if something unforeseen occurs during the time-step of one particle, the particle might fail to catch that event, resulting in a large integration error. A supernova (SN) explosion is an example of such an event. A SN generates a small amount of very hot gas ($T \sim 10^8$ K) in a large clump of cold gas ($T \sim 10$ K). The difference in the time-steps of the hot gas and surrounding cold gas particles becomes quite large (typically the difference reaches $\sim 10^3$). Thus, hot gas particles step forward $\sim 10^3$ or more time-steps before neighboring cold gas particles respond to the SN event. This means that the evolution of both hot and cold gas particles is completely wrong, since the surrounding cold gas particles do not react the explosion for a duration much longer than the timescale in which the blast wave would propagate the inter-particle distance. This problem is not severe for ordinary SPH simulations of galaxy formation because of the temperature cutoff in cooling functions at 10^4 K, while it becomes very serious for simulations involving the multiphase nature of the interstellar medium under 10^4 K, because the mach number can be very high.

This problem of sudden change occurs in any dynamical simulation with individual time-steps, as long as the time-steps are determined with the usual explicit method. In principle, a fully implicit method in which the time-step itself is also determined implicitly (Makino et al. 2006) or a method which satisfies Newton's third law (Farr & Bertschinger 2007) can solve this problem, but there are no implementations of such methods for SPH simulations yet [3].

In simulation of star clusters, the SN and its kick introduces a sudden change in the orbit (and mass) of the exploded star. Here, a rather simple prescription in which either all stars or at least nearby stars are synchronized to the time of explosion and restart the integration has been used. This prescription, at least the version which synchronizes all particles in the system, is impractical for N-body/SPH simulations of galaxies, because the number of SN events and therefore the increase in the calculation cost is too great.

We propose a simple limiter for hydrodynamical time-steps in the individual time-step method which mitigates this problem. With this limiter the behavior of an explosion integrated by individual time-steps becomes essentially the same as that integrated by global time-steps. In §2, we describe this limiter, and in §3 we report the result of numerical experiments.

2. THE TIME-STEP LIMITER

We denote the time-step of an i-th particle as dt_i and that of a neighbor particle, with index j, as dt_j. The basic idea of our limiter is to enforce the following conditions:

$$dt_i \leq f\ dt_j \quad \text{and,} \tag{1}$$

$$dt_j \leq f\ dt_i\ , \tag{2}$$

where f is an adjustable parameter. We found $f = 4$ to give good results, from the perspective of the total energy and linear momenta conservations, without significant increase in the calculation cost (see Table 1 in §3.2). Note that too large values of f, say $f > 4$, lead to the violation of the Courant condition. It is essential that the time-step of a particle j shrinks

Electronic address: saitoh.takayuki@nao.ac.jp,saitoh.takayuki@cfca.jp
[1] Center for Computational Astrophysics, National Astronomical Observatory of Japan, Mitaka, Tokyo 181-8588, Japan
[2] Division of Theoretical Astronomy, National Astronomical Observatory of Japan, 2–21–1 Osawa, Mitaka-shi, Tokyo 181–8588; and School of Physical Sciences, Graduate University of Advanced Study (SOKENDAI)

[3] Recently, Springel (2009) has developed a mesh-based scheme employing individual time-steps where the smaller time-step is adopted for integrations between neighboring meshes. This scheme does satisfy Newton's third law.

when the time-step of its neighbor particle i suddenly shrinks by a large factor. Thus particle i should let particle j respond to the change of its time-step. The key point of the limiter is to reduce effects of the violation of Newton's third law. Although our approach does not guarantee the third law, we can achieve sufficient accuracy by controlling the violation via the control parameter, f.

We implement this limiter in the following way: when integrated, particle i sends its new dt_i to its neighbor (j-th) particles. The particles receiving the time-step of particle i compare it with their time-steps, dt_j. When $dt_j > f\ dt_i$ they shorten their time-steps so that they satisfy the relation $dt_j = f\ dt_i$.

Note that this reduction of the time-step of particle j is only possible if the times of two particles t_i and t_j satisfy the condition

$$t_i \geq t_j + f\ dt_i. \tag{3}$$

If the above condition is not satisfied, the reduction of time-step results in the new time of particle j before the current time of particle i, requiring the backward integration of the entire system.

In this case, the new time of particle j is set to a value that is consistent with the current system time (t_i), and the time-step is set to the difference between particle' current time and new time. In Figure 1, we show schematic pictures of the traditional individual time-steps method and our implementation of the individual time-steps method.

3. NUMERICAL EXPERIMENTS

3.1. *Initial Setups and Method*

In order to verify the effect of the limiter, we performed two explosion tests. The first test deals with hydrodynamics only while the second one treats both hydrodynamics and self-gravity. For each test, we performed three runs: (a) integrated with global time-steps (hereafter Run a), (b) traditional individual time-steps (case 1. in Fig. 1; Run b), and (c) individual time-steps with the limiter (case 2. in Fig. 1; Run c).

For the first test we adopted the Sedov problem, which is a pure hydrodynamical evolution of the point-like explosion in the cold and homogeneous ambient medium (Sedov 1959). We prepared a glass distribution with 64^3 SPH particles. We enhanced the thermal energy of the central 32 particles in an SPH manner. The total thermal energy of the explosion is set to be unity. The internal energy of the ambient gas particle is set to be 10^{-6} of that for the hottest gas particle, although the original Sedov problem adopted a zero-energy background. Hence, the energy ratio is comparable with SN explosion, which generates a small amount of very hot gas ($T \sim 10^7$ K), in cold ($T \sim 10$ K) ambient gas. In this configuration, the position of the shock front at the time T is $\sim 1.15 \times T^{2/5}$, when we assume the adiabatic index $\gamma = 5/3$.

In figure 2, we show the initial distribution of time-steps for the Sedov problem with individual time-steps as a function of the radius. The difference in time-steps between the hottest particle and the ambient particles is $\sim 10^3$. Note that time-steps of particles in the contact region surrounding the hot region are smaller than those of distant ambient particles ($dt = 0.009$), since we estimate these time-steps after the internal energy of particles are specified. This distribution of time-steps is quite moderate compared to that in practical simulations just after SN explosions, in which only the particles which receive the energy have small time-steps.

We then perform an explosion test of a cold cloud including the self-gravity. For this test, we used the particle distribution of the three-dimensional collapse test (e.g., Evrard 1988) at $T = 3$ where the system becomes the state of virial equilibrium with the total energy of $E \sim -0.6$. We added the thermal energy to the central 32 particles in an SPH manner in order to drive the explosion of the system. The total energy of the system was set to be $E = 10$.

We designed this test to mimic the SN energy input in high-density star-forming molecular cloud. The total binding energy of a cloud with the total mass of $10^4\ M_\odot$ and the size of 10 pc (see Table 1 in Bergin & Tafalla 2007) is around -10^{48} ergs, while the energy input of a type II SN is 10^{51} ergs. Therefore, if we scale the energy accordingly, the energy input should be ~ 600. We used a much smaller value, so that the breakdown of the traditional method is less severe. We reset $T = 0$ at the initial state. The number of SPH particles used here is 30976. The gravitational softening, ϵ, is set to be 0.05.

We use the standard SPH method (e.g., Monaghan 1992). The asymmetric form is adopted for the derivation of the internal energy. The signal velocity based artificial viscosity term (Monaghan 1997) is used. The viscous coefficient, α, is set to be two for the first test and unity for the second test. We determine the interaction (kernel) size of each SPH particle to keep the neighbor number to 32 ± 2. Gravity is solved by the Tree with GRAPE method (Makino 1991b) with an opening angle of 0.5.

The time-integrator uses the leap-frog method. In runs of pure hydrodynamics, the time-step for individual particles is calculated as the smaller of the ones calculated using the signal velocity based method (Monaghan 1997; Springel 2005) and the acceleration time-step; $0.3 \times (2h/|a_{\rm h}|)^{0.5}$ (Monaghan 1992). Here h and $a_{\rm h}$ are the kernel size and the acceleration caused by the pressure gradient, respectively. The coefficient for the Courant condition, which is estimated by the signal velocity based method, is set to be 0.3. When we consider self-gravity, we modify the acceleration time-step taking into account the gravitational acceleration, $a_{\rm g}$, and ϵ; $0.3 \times (\min(2\ h, \epsilon)/|a_{\rm h} + a_{\rm g}|)^{0.5}$.

3.2. *Results*

Figure 3 shows the result of the Sedov problem. In the top row, particle distributions of sliced regions ($|z| < 0.01$) are shown, and in the bottom row radial density profiles are shown. Run (a) (the left panels in Fig. 3) shows a clear spherical structure and its density profile traces the analytic solution very well.

Run (b) (the middle panels), however, displays penetrations of the hot gas particles into the ambient medium and fails to reproduce the analytic solution. This is because the time-steps of the gas particles composing the ambient medium are very long ($dt \sim 10^{-2}$) compared with those of the initially heated particles (the minimum value is $dt \sim 10^{-5}$) and therefore the ambient medium has had only two time-steps before the time of the snapshot ($T = 0.02$). They could not respond correctly to the expansion of the central hot region.

Run (c) (the right panels) does not show this problem. In this run, the penetration of the hot gas particle occurring with the traditional method is suppressed perfectly and the analytic solution of the Sedov problem is reproduced very well. This is because the short time-steps propagate to surrounding particles quickly enough. As a result, cold gas particles can respond to the pressure of the hot gas particles. Conse-

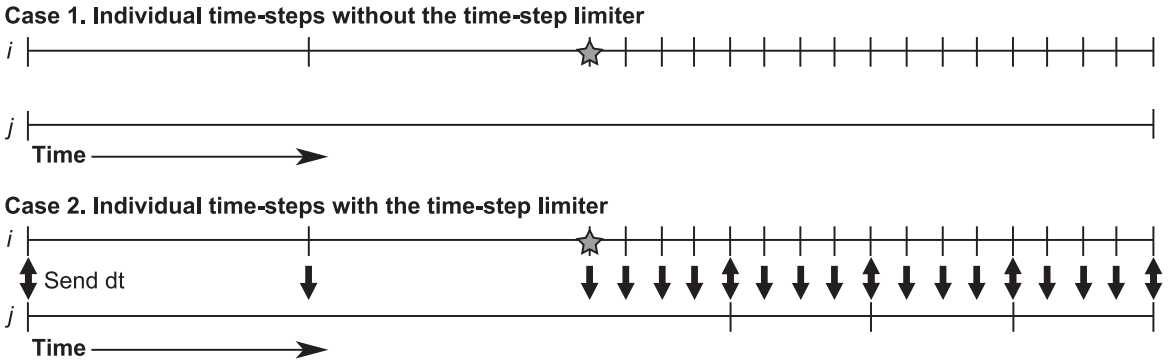

FIG. 1.— Schematic pictures of individual time-step methods without and with the time-step limiter (case 1. and 2.). Particle i suddenly shrinks its time-step (dt_i) at the time indicated by the star symbol. In case 1., particle j does not respond to the change of dt_i. In case 2., particles i and j always send their time-steps (dt_i and dt_j) to their neighbors when they become active. If the minimum time-step of neighbors is shorter than its own time-step by a factor f (see text), a particle shortens its time-step.

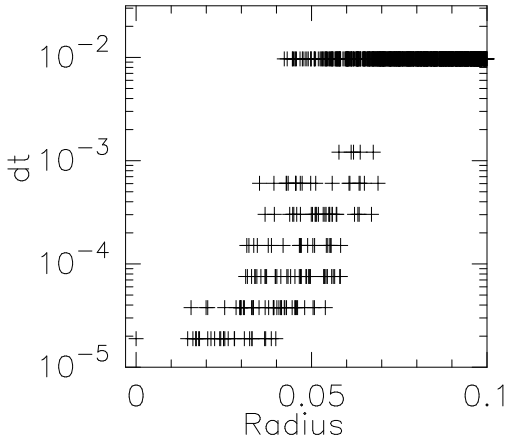

FIG. 2.— The distribution of initial time-steps for the Sedov problem with individual time-steps as a function of the radius.

quently this run can reproduce the analytic solution of the Sedov problem, like Run (a). We can conclude that this limiter or a similar criterion is necessary for the simulations of SPH with individual time-steps involving strong explosions.

The total (kinetic + thermal) energy and linear momenta of the system at the final phase ($T = 0.04$) are shown in Table 1. Run (a) conserves the total energy to $\sim 10^{-3}$ and the linear momentum with a very high precision. While Run (b) shows violations of conservation of both the total energy and the linear momentum because the time-steps of cold gas particles are far too long to resolve the propagation of the blast wave.

Introduction of the time-step limiter greatly reduces these errors. Runs (c) conserve the total energy to a level similar to that of Run (a). In addition, the conservations of the linear momentum in these runs are improved by four orders of magnitudes compared with that in run (b). When we compare runs with $f = 2$ and 4, we found the run with $f = 2$ shows results slightly better in conservations. The distribution of particles and radial profiles are indistinguishable. Therefore we conclude that the time-step limiter with $f = 4$ is acceptable.

The calculation cost directly relates with the value of f; smaller f leads to larger calculation cost. Indeed, Run (c) with $f = 2$ takes 1036 sec for integration until $T = 0.4$ whereas Run (c) with $f = 4$ requires only 489 sec. Interestingly, calculation costs for Runs (c) are smaller than that for Run (b). This is because the hot bubble does not expand correctly unless we introduce the limiter.

TABLE 1
ENERGY AND MOMENTUM CONSERVATION AND CALCULATION COST.

Run	$\lvert(E_I-E_F)/E_I\rvert$	$\lvert p_F\rvert_x$	$\lvert p_F\rvert_y$	$\lvert p_F\rvert_z$	Time (sec)
a	8.2e-4	1.4e-16	1.4e-15	7.7e-16	5646
b	7.2	5.4e-1	2.6e-1	3.1e-1	2068
c($f = 2$)	7.6e-4	3.2e-5	3.1e-5	1.1e-5	1036
c($f = 4$)	5.9e-3	1.7e-5	2.7e-5	2.2e-6	489

Note. E_I and E_F are the total energy at $T = 0$ (initial phase) and 0.04 (final phase), respectively. $|p_F|_x$, $|p_F|_y$, and $|p_F|_z$ indicate the absolute values of linear momenta for x, y, and z directions, respectively.

Figure 4 shows sliced ($|z| < 0.2$) particle distributions for Runs (a), (b), and (c) (top to bottom) at selected epochs, for the second model with self-gravity. Since the total (kinetic + thermal + potential) energy of the system is positive and sufficiently large, the strong shock propagates outward against the self-gravity resulting in an expanding shell. Run (a) (top panels) shows this behaviors clearly. The behavior of the expansion for Run (b) (middle panels) surprisingly differs from that for run (a). Again, the penetrations of the initial hot gas particles into the cold region are observed, and defects of the shell are shown in the middle-center and right panels. The introduction of the time-step limiter drastically improves the results as can be seen in the bottom panels of Figure 4. There are no penetrations or defects of the spherical shell-like shock which are visible in middle panels.

These results clearly indicate that the use of individual time-steps without a time-step limiter is very dangerous for SPH simulations involving strong explosion problems, such as high-resolution SPH simulations of galaxy formation with a multiphase interstellar medium under 10^4 K. On the other hand, for traditional simulations of galaxy formation, the problem might not be too severe since these simulations adopt the cut off temperature of 10^4 K for cooling function, and temperature difference is at most around 100. We strongly recommend that users of SPH who investigate systems in which "strong" explosions take place with individual time-steps implement some form of time-step limiter similar to what we introduced here.

We thank the anonymous referee for his/her insightful comments and suggestions, which helped us to greatly improve our manuscript. We also thank Takashi Okamoto for helpful discussion and Kohji Yoshikawa for providing us with a custom version of Phantom-GRAPE library. Numerical com-

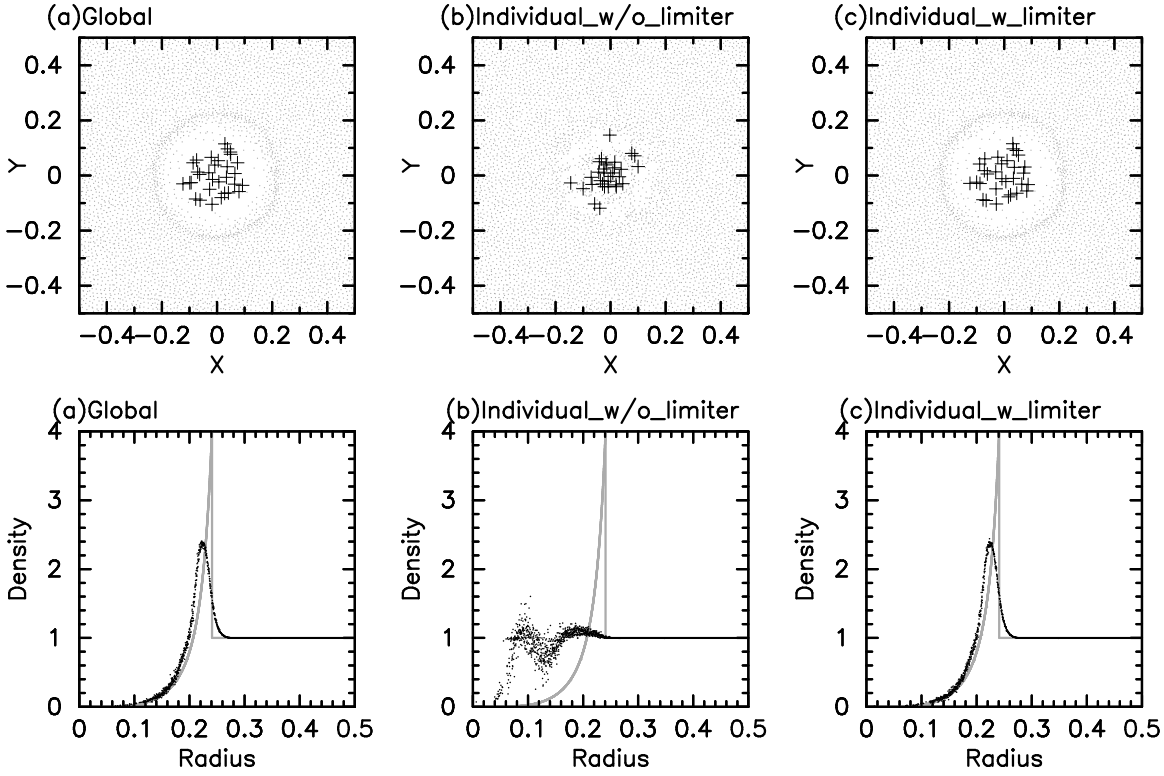

FIG. 3.— Left, middle, and right column of panels show the evolution of particles integrated with (a) global time-steps, (b) individual time-steps, and (c) individual time-steps and the time-step limiter, respectively. The upper row shows particle distributions for three runs at $T = 0.02$. Points indicate projected positions of SPH particles in sliced regions ($|z| < 0.01$) while crosses show those of initially heated SPH particles throughout whole regions. The lower row shows radial density profiles for three runs at $T = 0.02$. Points show geometrical means of densities for every radial bin with the width of 0.005 from the origin of coordinates. Solid (gray) curves are the analytic solution for the zero-energy background obtained by Sedov (1959).

putations were carried out on XT-4/GRAPE systems (project ID:g08a19) at the Center for Computational Astrophysics, CfCA, of the National Astronomical Observatory of Japan.

REFERENCES

Bergin, E. A., & Tafalla, M. 2007, ARA&A, 45, 339
Evrard, A. E. 1988, MNRAS, 235, 911
Farr, W. M., & Bertschinger, E. 2007, ApJ, 663, 1420
Gingold, R. A., & Monaghan, J. J. 1977, MNRAS, 181, 375
Hernquist, L., & Katz, N. 1989, ApJS, 70, 419
Lucy, L. B. 1977, AJ, 82, 1013
Makino, J. 1991a, PASJ, 43, 859
—. 1991b, PASJ, 43, 621
Makino, J., Hut, P., Kaplan, M., & Saygın, H. 2006, New Astronomy, 12, 124
McMillan, S. L. W. 1986, in Lecture Notes in Physics, Berlin Springer Verlag, Vol. 267, The Use of Supercomputers in Stellar Dynamics, ed. P. Hut & S. L. W. McMillan, 156–+
Monaghan, J. J. 1992, ARA&A, 30, 543
—. 1997, Journal of Computational Physics, 136, 298
Sedov, L. I. 1959, Similarity and Dimensional Methods in Mechanics (Similarity and Dimensional Methods in Mechanics, New York: Academic Press, 1959)
Springel, V. 2005, MNRAS, 364, 1105
—. 2009, ArXiv e-prints, 0901.4107

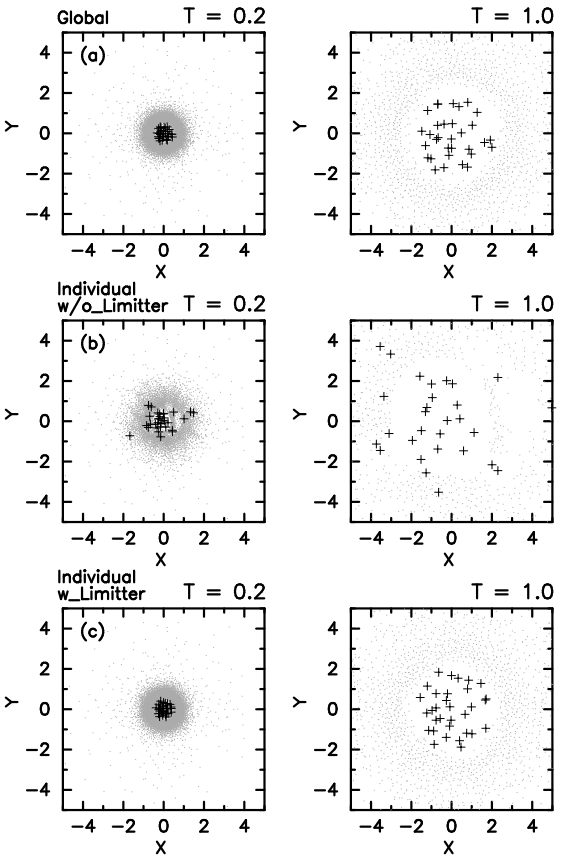

FIG. 4.— Evolution of particles for three runs. Upper, middle, and lower rows of panels show the evolution of particles integrated with (a) global time-steps, (b) individual time-steps, and (c) individual time-steps and the time-step limiter, respectively. Points and crosses indicate projected positions of SPH particles in sliced regions ($|z| < 0.2$) and those of initially heated SPH particles in whole regions, respectively.